Hall and ion-slip effects on the unsteady MHD mixed convection of Cu-water nanofluid over a vertical stretching plate with convective heat flux

Xiaohong Su*

School of Mathematics and Physics, North China Electric Power University,

Baoding 071 003, China

The problem of unsteady MHD mixed convective flow of a Cu-water nanofluid over a vertical convectively heated plate has been analyzed. The effects of Hall and ion-slip currents have also been taken into consideration. The governing nonlinear partial differential equations have been reduced to a system of nonlinear coupled similarity equations. The resulting similarity equations have been solved numerically to obtain the axial velocity, transverse velocity and temperature in the corresponding boundary layers. It has been found that the variations of the Hall and ion-slip parameters can remarkably affect the velocity and temperature distributions of the nanofluid. Further, the transfer characteristics of the axial velocity, the transverse velocity and the temperature of Cu-water nanofluid under various values of unsteadiness parameter, magnetic parameter, the boundary convection parameter and the mixed convection parameter have been described and discussed, respectively.

Keywords: Unsteady MHD flow, Heat transfer, Analytical solution, Slip condition

1 Introduction

Researchers and scientists are interested in exploring the fluid medium with high heat transfer efficiency in view of its applications in many energy technologies. Nanofluids are a new kind of heat transfer fluids. These fluids are colloidal suspensions containing nanoparticles in a common base fluid. Nanofluids offer an innovative idea in improving heat transfer performance of the traditional heat transfer fluids and have promising applications. Thus nanofluids become one of the focus areas in recently engineering and science researches. The nanoparticles used in nanofluids are typically made of metals (e.g., silver, copper and gold), oxides, and so on. The common base fluids include oil, ethylene glycol mixture and water. In the recent researches related on nanofluids, various investigations have been made to study the behaviors of convective flow of nanofluids. Tzou[1-2] analyzed the thermal instability of nanofluids in natural convection. Alloui et al.[3] recently presented a study on natural convection of nanofluids in a shallow rectangular cavity. Freidoonimehr et al.[4] investigated the transient MHD natural convection of four different types of water based nanofluids (Cu, CuO, Al_2O_3, TiO_2) past a vertical plate. The problem of the natural convection of a nanofluid over an isothermal vertical plate was explored by Kuznetsov and Nield[5].

The convective boundary condition extends the conditions of the common constant temperature or heat flux at the plate surface. The use of the thermal convective boundary condition was first introduced by Aziz[6] in studying Blasius flow over a flat plate. After his pioneering work, the nanofluid flow and heat transfer with a convective boundary condition have also been explored by some authors. Aziz and Khan[7] studied the effect of a convective boundary condition on the natural convective flow of a nanofluid over a vertical plate. Yacob et al.[8] numerically studied boundary layer flow of nanofluid past a stretching/shrinking plate beneath an external uniform shear flow with a convective boundary condition. The boundary layer flow of a nanofluid induced by a linearly stretching sheet with a convective heat flux was studied numerically by Makinde and Aziz[9].

Convection over a cooled or heated plate is one of the fundamental problems in the studies on flow and heat transfer of fluids[10]. The combined flow, in which free and forced convection exists, is commonly called as a mixed convection flow. Subhashini et al.[11] studied the mixed convection flow of nanofluids near the stagnation point region. Among the alumina-water nanofluid, the copper-water nanofluid and the base fluid, they revealed that the copper-water nanofluid has

*E-mail: suxh2005@163.com

the highest value of the heat transfer rate and the skin friction coefficient at the plate. The characteristics of mixed convective flow over a stretching vertical sheet, which is immersed in a nanofluid, were investigated numerically by Yacob et al.[12]. Magnetic fields have important applications in many engineering devices such as MHD generator nuclear reactors, plasma studies, geothermal extractions, and the boundary layer control in the field of aeronautics and aerodynamics. Researchers have tried to explore the influences of magnetic fields on the flow and heat transfer behaviors of nanofluid in the mixed convection. Sheikholeslami et al.[13] investigated MHD natural convection heat transfer of nanofluid in a concentric annulus by using lattice Boltzmann method. Hatami et al.[14] analyzed the MHD forced convection of Al_2O_3-water nanofluid over a stretching horizontal plate. Yazdi et al.[15] presented the mixed convection over a stretching vertical plate in porous medium filled with nanofluid in the presence of a magnetic field.

In most of the above papers cited earlier, the effects of the Hall and ion-slip currents were neglected in applying Ohm's law[16]. The main reason lies in that the Hall and ion-slip currents have no significant effect for the relatively weak magnetic field. On the other hand, the strong magnetic fields are more and more widely utilized in the application of magneto-hydrodynamics. In these cases where electromagnetic force is noticeable, the Hall and ion-slip currents have remarkable effects for the transfer of the momentum and energy of fluids. Hence, the studies on the flow and heat transfer of fluids with taking into account Hall or ion-slip currents are of great importance. In recent years, some investigators have focused on this research field. Megahed et al.[17] investigated the Hall effects on free convection flow and mass transfer past a semi-infinite vertical flat plate. Srnivasacharya and Shiferaw[18] presented a boundary layer analysis about the combined effects of Hall and ion-slip currents on MHD flow of micropolar fluid in a rectangular duct. Srinivasacharya and Kaladhar[19] studied the Hall and ion-slip effects on fully developed electrically conducting couple stress fluid flow between vertical parallel plates. In the investigation of the peristaltic flow and heat transfer of an incompressible and electrically conducting viscous fluid in a two-dimensional asymmetric channel, Asghar et al.[20] also took into account the Hall and ion-slip effects. Su et al.[21] studied the effect of Hall current on the boundary layer flow and heat transfer of the nanofluids over a stretching wedge by means of a numerical method.

Makinde et al.[22] reported the hydromagnetic Couette-Poiseuille flow of nanofluids with heat and mass transfer between two parallel plates in a rotating permeable channel. Their results show that Hall current significantly affects the flow system. The combined influences of Hall current and chemical reaction on the mixed convective peristaltic flow of Prandtl fluid in asymmetric channel were analyzed by Hayat et al.[24] in which they addressed the Hall and ion slip effects on peristaltic flow of Jeffrey nanofluid. They found the velocity increases and temperature decreases with Hall and ion slip parameters in the flow of Jeffrey nanofluid.

Keeping in mind all of the above mentioned investigations, the aim here is to analyze the MHD mixed convection of the Cu-water nanofluid over a vertical unsteady stretching sheet with a heat flux. The effects of the Hall and ion-slip currents are taken into account. To the best of my knowledge, such study has not appeared in literatures. According to the results obtained by a numerical method, the combined effects of the related physical parameters will be presented in detail in this paper.

2 Mathematical Formulations

The MHD mixed convection of a Cu-water nanofluid over an unsteady stretching vertical plate with a heat flux has been considered in the presence of a variable strong magnetic field. The physical description and coordinate system of this flow are shown in Fig. 1. The stretching direction of the plate is along the x-axis and is normal to the y-axis. The z-axis is transverse to the xy-plane. The stretching velocity of the plate is $u_w = ax(1-ct)^{-1}$. Here t is the
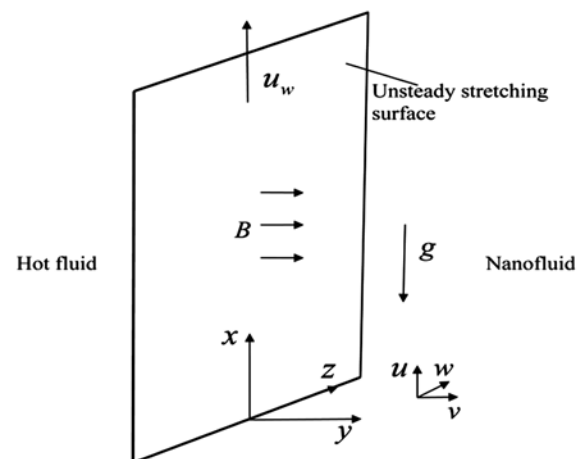

Fig. 1 – A physical description of the problem.

time, a and c are two positive constants satisfying $ct < 1$ and having the dimension $(\text{time})^{-1}$. The velocity of the nanofluid far away from the plate is zero. The back side of the vertical plate is in contact with a hot fluid maintaining a temperature $T_{\text{f}} = T_{\infty} + ax^2(2\nu)^{-1}(1 - ct)^{-2}$ in which T_{∞} is the temperature of the nanofluid outside the boundary layer. The flow of the Cu-water nanofluid is under the influence of a variable strong magnetic field $\mathbf{B} = (0, B, 0)$ in which $B = B_0 u_w^{1/2}(\nu x)^{-1/2}$. The induced magnetic field can be negligible by assuming that the flow of nanofluid is performed under the low magnetic Reynolds number. A force is produced along the z-axis and then gives rise to a cross flow in the direction of the z-axis by Hall effect duo to the variable strong magnetic field. Assuming that the plate has very large width in the direction of the z-axis, the nanofluid can be considered to have the same flow quantities along the z-direction. Based on the flow situation described above, the generalized Ohm's law[16] with Hall and ion-slip effects is given by:

$$\mathbf{J} = \sigma(\mathbf{E} + \mathbf{V} \times \mathbf{B}) - \frac{\omega_e \tau_e}{B}(\mathbf{J} \times \mathbf{B}) \qquad \dots (1)$$

$$+ \frac{\omega_e \tau_e Bi}{B^2}((\mathbf{J} \times \mathbf{B}) \times \mathbf{B})$$

where $\mathbf{J} = (J_x, J_y, J_z)$ is the current density vector, τ_e is the electrical collision time, ω_e is the electron frequency, Bi is the ion-slip parameter, $\mathbf{E}$ is the intensity vector of the electric field, $\mathbf{V}$ is the velocity vector. The plate is assumed to be electrically insulating, which gives rise to $J_y = 0$ in the flow field. Then by using the Maxwell equation and Eq. (1), the current density vector becomes:

$$\mathbf{J} = \frac{\sigma B}{((1 + BiBe)^2 + Be^2)}(Beu - (1 + BiBe)w, \qquad \dots (2)$$

$$0, (1 + BiBe)u + Beu)$$

in which $Be = \omega_e \tau_e$ is the Hall parameter. Further, from Eq. (2), the Lorentz force can be expressed as follows:

$$\mathbf{J} \times \mathbf{B} = \frac{\sigma B^2}{((1 + BiBe)^2 + Be^2)}(-(1 + BiBe)u \qquad \dots (3)$$

$$- Bew, 0, Beu - (1 + BiBe)w)$$

Considering the Lorentz force Eq. (3), we may give the boundary layer *governing equations for the* momentum and energy conservation of the nanofluid by:

$$\frac{\partial u}{\partial x} + \frac{\partial v}{\partial y} = 0 \qquad \dots (4)$$

$$\frac{\partial u}{\partial t} + u\frac{\partial u}{\partial x} + v\frac{\partial u}{\partial y} = \frac{\mu_{\text{nf}}}{\rho_{\text{nf}}}\frac{\partial^2 u}{\partial y^2}$$

$$- \frac{\sigma B^2}{\rho_{\text{nf}}((1 + BiBe)^2 + Be^2)}[(1 + BiBe)u \qquad \dots (5)$$

$$+ Bew] + g\beta_{\text{nf}}(T - T_{\infty})$$

$$\frac{\partial w}{\partial t} + u\frac{\partial w}{\partial x} + v\frac{\partial w}{\partial y} = \frac{\mu_{\text{nf}}}{\rho_{\text{nf}}}\frac{\partial^2 w}{\partial y^2}$$

$$+ \frac{\sigma B^2}{\rho_{\text{nf}}((1 + BiBe)^2 + Be^2)}[Beu \qquad \dots (6)$$

$$- (1 + BiBe)w],$$

$$\frac{\partial T}{\partial t} + u\frac{\partial T}{\partial x} + v\frac{\partial T}{\partial y} = \frac{k_{\text{nf}}}{(\rho C_p)_{\text{nf}}}\frac{\partial^2 T}{\partial y^2} \qquad \dots (7)$$

Here u, v and w are the x-, y- and z-components of the nanofluid velocity, T is the temperature, g is the acceleration of gravity. The above physical quantities of Cu-water nanofluid in Eqs (5-7) are defined as[13,25]:

$$\mu_{\text{nf}} = \frac{\mu_{\text{f}}}{(1 - \phi)^{2.5}}, \beta_{\text{nf}} = (1 - \phi)\beta_{\text{f}} + \phi\beta_{\text{s}},$$

$$\rho_{\text{nf}} = (1 - \phi)\rho_{\text{f}} + \phi\rho_{\text{s}}, \qquad \dots (8)$$

$$k_{\text{nf}} = \frac{(k_{\text{s}} + 2k_{\text{f}}) - 2\phi(k_{\text{f}} - k_{\text{s}})}{(k_{\text{s}} + 2k_{\text{f}}) + \phi(k_{\text{f}} - k_{\text{s}})}k_{\text{f}},$$

$$(\rho C_p)_{\text{nf}} = (1 - \phi)(\rho C_p)_{\text{f}} + \phi(\rho C_p)_{\text{s}}$$

In Eq. (8), ϕ is the Cu nanoparticle volume fraction. The above symbols $\mu, \beta, \rho, \rho C_p$ and k denote the viscosity, the volumetric coefficient of thermal expansion, the density, the heat capacity and the thermal conductivity. The above quantities (subscript s) and those (subscript f) represent the corresponding physical quantities of the Cu nanoparticle and those of the base fluid, respectively. The quantities (subscript nf) correspond to the physical quantities of the nanofluid. The case when $\phi = 0$ corresponds to the regular Newtonian fluid. In addition, the thermo-physical properties of Cu nanoparticle and water are shown in Table 1.

Table 1 – Thermophysical properties of Water and Cu nanoparticles[27]

	ρ (Kg m^{-3})	C_p (JKg^{-1}K^{-1})	k (Wm^{-1}K^{-1})	$\beta \times 10^{-5}$ (K^{-1})
H$_2$O	997.1	4179	0.613	21
Cu	8933	385	401	1.67

The boundary conditions for Eqs (4-7) are:

$$u = u_w, v = 0, w = 0,$$
$$-k \frac{\partial T}{\partial y} = h_f (T_f - T) \quad \text{at } y = 0, \quad \dots (9)$$

$$u = 0, \ w = 0, \ T = T_\infty, \text{as } y = \infty \quad \dots (10)$$

where the heat transfer coefficient h_f is proportional to $(1 - ct)^{-1/2}$.

To facilitate the analysis, we introduce the below dimensionless variables:

$$\eta = u_w^{\frac{1}{2}} (vx)^{-\frac{1}{2}} y, \ \psi(x,y) = (vxu_w)^{1/2} f(\eta),$$
$$w = u_w g(\eta), \ \theta(\eta) = \frac{T - T_\infty}{T_f - T_\infty} \quad \dots (11)$$

Here $\psi(x,y)$ is the stream function defined as $u = \partial\psi / \partial y$ and $v = -\partial\psi / \partial x$ so that the continuity Eq. (4) is automatically satisfied. In terms of the variables (Eq. (11)), Eqs (4-7) are transformed into:

$$f''' + ((1-\phi) + \phi\frac{\rho_s}{\rho_f}(1-\phi)^{2.5})(ff'' - f'^2)$$
$$- Af' - \frac{\eta A}{2} f'') - \frac{(1-\phi)^{2.5}M}{(1+BiBe)^2 + Be^2}((1 \quad \dots (12)$$
$$+ BiBe)f' + Beg) + ((1-\phi)$$
$$+ \phi\frac{(\rho\beta)_s}{(\rho\beta)_f})(1-\phi)^{2.5}\gamma\theta = 0$$

$$g'' + ((1-\phi) + \phi\frac{\rho_s}{\rho_f}(1-\phi)^{2.5})(fg' - f'g)$$
$$- Ag - \frac{\eta A}{2} g') + \frac{(1-\phi)^{2.5}M}{(1+BiBe)^2 + Be^2}(Bef' \quad \dots (13)$$
$$- (1 + BiBe)g) = 0$$

$$Pr^{-1} \frac{1}{(1-\phi) + \phi\frac{(\rho C_p)_s}{(\rho C_p)_f}} \frac{k_{nf}}{k_f} \theta'' - \frac{A}{2}\eta\theta' \quad \dots (14)$$
$$+ f\theta' - 2\theta f' - 2A\theta = 0$$

where the functions $f'(\eta) = u / u_w$, $g(\eta) = w / u_w$ and θ represent the dimensionless axial velocity, transverse velocity and temperature, respectively.

The reduced boundary conditions are:

$$f(0) = 0, f'(0) = 1, g(0) = 0,$$
$$\theta'(0) = -\lambda[1 - \theta(0)], \quad \dots (15)$$
$$f'(\infty) = 0, g(\infty) = 0, \theta(\infty) = 0$$

In the Eqs (12-14), $A = c/a$ is the unsteadiness parameter and can be obviously used to measure the unsteadiness of this flow[26]. The case when $A = 0$ corresponds to the traditional steady flow. The Prandtl number Pr, the local Reynolds number Re_x, the magnetic parameter M, the mixed convection parameter γ and the boundary convection parameter λ are respectively defined as:

$$Pr = \frac{v_f}{\alpha_f}, Re_x = \frac{u_w x}{v_f}, M = \frac{\sigma B_0^2}{\rho_f v} \quad \dots (16)$$
$$\gamma = \frac{g\beta_f(T_w - T_\infty)x^3}{v^2}, \lambda = \frac{h_f}{k_f}\sqrt{\frac{2vx}{u_w}}$$

The physical quantities of primary interest include C_{fx} and C_{fz}, which are the local skin friction coefficients in the x- and z- directions, and the local Nusselt number Nu_x. These quantities denote the shear stress at the plate and the heat transfer rate which are presented in the following Eqs (17,18), respectively.

The local skin friction coefficients C_{fx} and C_{fz} are expressed as:

$$C_{fx} = \frac{\mu_{nf}}{\rho_f u_w^2}(\frac{\partial u}{\partial y})_{y=0} = \frac{1}{(1-\phi)^{2.5}} Re_x^{-\frac{1}{2}} f''(0), \text{i.e.}$$

$$C_{fx} Re_x^{\frac{1}{2}} = \frac{1}{(1-\phi)^{2.5}} f''(0), \quad \dots (17)$$

$$C_{fz} = \frac{\mu_{nf}}{\rho_f u_w^2}(\frac{\partial w}{\partial y})_{y=0} = \frac{1}{(1-\phi)^{2.5}} Re_x^{-\frac{1}{2}} g'(0), \text{i.e.}$$

$$C_{fz} Re_x^{\frac{1}{2}} = \frac{1}{(1-\phi)^{2.5}} g'(0)$$

The local heat transfer rate in terms of Nusselt number is defined by:

$$Nu_x = -\frac{k_{nf}x}{k_f(T_w - T_\infty)}(\frac{\partial T}{\partial y})_{y=0}$$

$$= -\frac{k_{nf}}{k_f} Re_x^{\frac{1}{2}} \theta'(0), \text{i.e.} \qquad \dots (18)$$

$$Nu_x Re_x^{-\frac{1}{2}} = -\frac{k_{nf}}{k_f} \theta'(0)$$

3 Method of Solution

The nonlinear coupled differential similarity Eqs (12-14) with the boundary condition (Eq. (15)) are solved numerically. The numerical method used in this paper is the fourth order Runge-Kutta method along with the shooting technique. This approach was used successfully[21] and its accuracy has been verified by us. To be specific, the Eqs (12-14) are first converted into the following system of first-order differential equations:

$$f_1' = f_2, f_2' = f_3, f_4' = f_5, f_6' = f_7,$$

$$f_3' = -((1-\phi) + \phi\frac{\rho_s}{\rho_f}(1-\phi)^{2.5})(f_1 f_3 - f_2^2$$

$$- Af_2 - \frac{\eta A}{2}f_3) + \frac{(1-\phi)^{2.5}M}{(1+BiBe)^2 + Be^2}((1$$

$$+ BiBe)f_2 + Bef_4) - ((1-\phi)$$

$$+ \phi\frac{(\rho\beta)_s}{(\rho\beta)_f})(1-\phi)^{2.5}\gamma f_6,$$

$$f_5' = -((1-\phi) + \phi\frac{\rho_s}{\rho_f}(1-\phi)^{2.5})(f_1 f_5 - f_2 f_4$$

$$- Af_4 - \frac{\eta A}{2}f_5) + \frac{(1-\phi)^{2.5}M}{(1+BiBe)^2 + Be^2}(Bef_2$$

$$- (1+BiBe)f_4)$$

$$f_7' = Pr((1-\phi) + \phi\frac{(\rho C_p)_s}{(\rho C_p)_f})\frac{k_f}{k_{nf}}(\frac{A}{2}\eta f_7 \qquad \dots (19)$$

$$- f_1 f_7 + 2f_6 f_2 + 2Af_6),$$

where $f = f_1$, $g = f_4$, $\theta = f_6$. Next, according to the boundary condition (Eq. (15)), the below initial conditions are introduced:

$$f_1(0) = 0, f_2(0) = 1, f_3(0) = \alpha_1,$$

$$f_4(0) = 0, f_5(0) = \alpha_2, \qquad \dots (20)$$

$$f_6(0) = \alpha_3, f_7(0) = -\lambda(1-\alpha_3).$$

After the suitable initial guess values for α_1, α_2 and α_3 are chosen, the initial value problem Eqs (19,20) are solved repeatedly by using the fourth-order Runge-

kutta technique with the secant method. The step size $\Delta\eta$ is chosen as 0.001. When the boundary conditions $f'(\eta_\infty) = 0$, $g(\eta_\infty) = 0$ and $\theta(\eta_\infty) = 0$, are satisfied with an accuracy of below 10^{-4}, the iteration calculation stops.

4 Results and Discussion

Computations have been implemented for various values of the unsteadiness parameter A, the nanoparticle volume fraction ϕ, the Hall parameter Be, the ion-slip parameter Bi, the magnetic parameter M, the boundary convection parameter λ and the mixed convection parameter γ. By means of solving the above governing equations, the dimensionless axial velocity, transverse velocity and temperature distributions corresponding to various values of the parameters are presented in Figs 2-22. All the transverse velocity profiles reflect a common feature that the transverse velocity $g(\eta)$ monotonically goes up to a peak value and then monotonically decreases to zero. The other characteristics under various values of the above mentioned parameters are elaborated in the following paragraphs, respectively.

The distributions of the axial velocity $f'(\eta)$, transverse velocity $g(\eta)$ and temperature $\theta(\eta)$ for different values of the unsteadiness parameter A are given in Figs 2-4. From these figures, it can be drawn that the effect of increasing values of the unsteadiness parameter is to decrease the axial velocity $f'(\eta)$, the peak value of the transverse velocity $g(\eta)$ and the temperature in the boundary layer of nanofluid. Moreover, Fig. 4 obviously shows that the temperature boundary layer becomes thinner as the unsteadiness parameter increases.

Now the attention is paid to how the Cu nanoparticle volume fraction ϕ affects the velocities $f'(\eta)$, $g(\eta)$ and temperature $\theta(\eta)$. In Figs 5, 6 and 7, the variation of the Cu nanoparticle volume fraction ϕ produces obvious effects on the velocity and temperature distributions of nanofluid. It is observed from Figs 5 and 7 that both the axial velocity $f'(\eta)$ and the temperature increase with the increasing of ϕ. Figure 6 reveals that an increase in the Cu nanoparticle volume fraction leads to a decrease of the peak value of the transverse velocity $g(\eta)$. In addition, compared with the pure base fluid (i.e., $\phi = 0$), the Cu-water

nanofluid provides the higher heat transfer rate, and this feature becomes more evident as the Cu nanoparticle volume fraction increases.
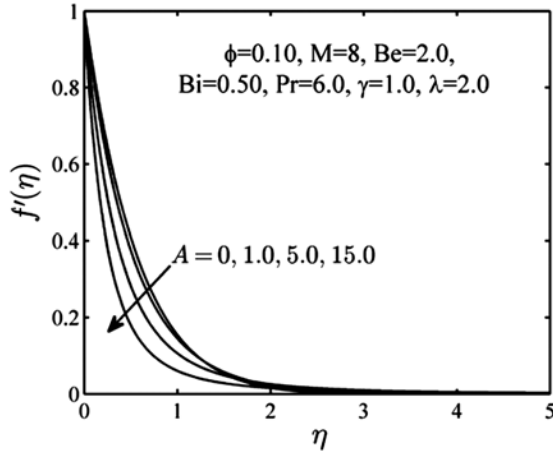

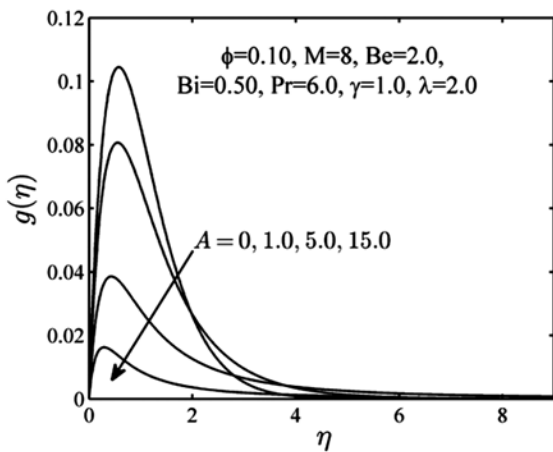Fig. 2 – Effect of A on axial velocity profiles.

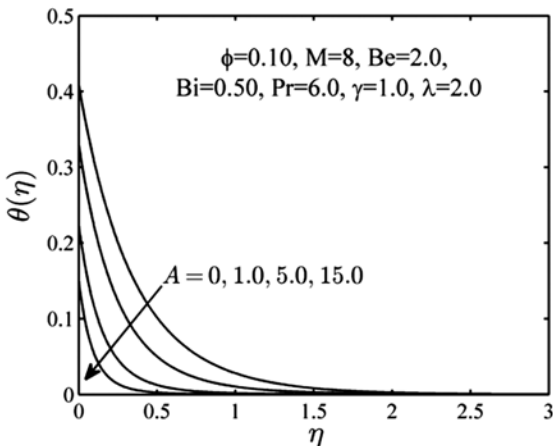Fig. 3 – Effect of A on transverse velocity profiles.

Fig. 4 – Effect of A on temperature profiles.

Figures 8, 9 and 10 are drawn to exhibit the influences of Hall parameter Be on the velocities $f'(\eta)$, $g(\eta)$ and temperature $\theta(\eta)$ of nanofluid, respectively. By increasing the value of Be, we observe that the axial velocity $f'(\eta)$ increases, but at the same time the temperature $\theta(\eta)$ decreases. Figure 9 presents a conclusion that the maximum value of the transverse velocity $g(\eta)$ first increases and then decreases as Be continuously increases.

Figures 11, 12 and 13 show the variation in the distributions of the velocities $f'(\eta)$, $g(\eta)$ and temperature $\theta(\eta)$ of nanofluid by increasing the value of the ion-slip parameter Bi, respectively. Figure 11 reveals that the axial velocity $f'(\eta)$ increases with the increase in Bi. This behavior can be deduced from Fig. 12 that the transverse velocity $g(\eta)$ decreases with an increment in Bi. From Fig. 13, we observe that an increase in the
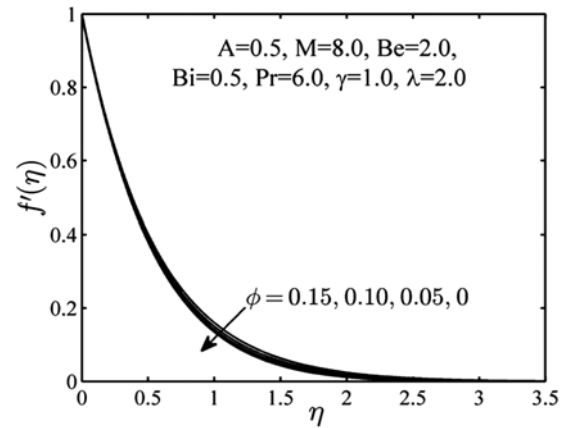
Fig. 5 – Effect of ϕ on axial velocity profiles.
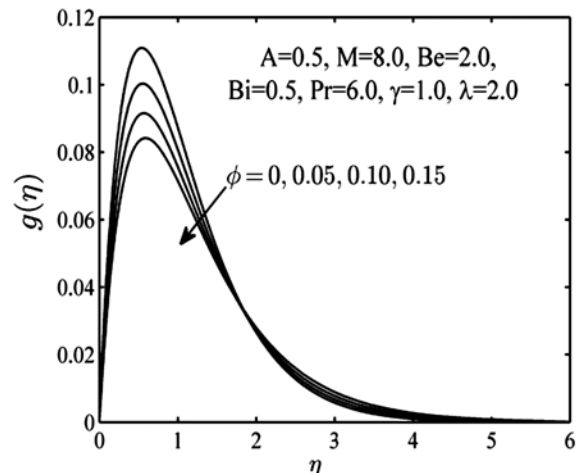
Fig. 6 – Effect of ϕ on transverse velocity profiles.

ion-slip parameter causes a small reduction of the temperature $\theta(\eta)$ of the nanofluid in the boundary layer.

Figures 14, 15 and 16 indicate the influence of magnetic parameter M on the flow and heat transfer of

the Cu-water nanofluid. It can be seen that the axial velocity $f'(\eta)$ and its boundary layer thickness obviously decrease with magnetic parameter M
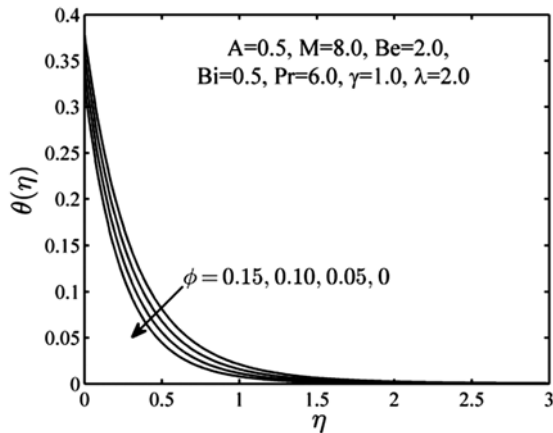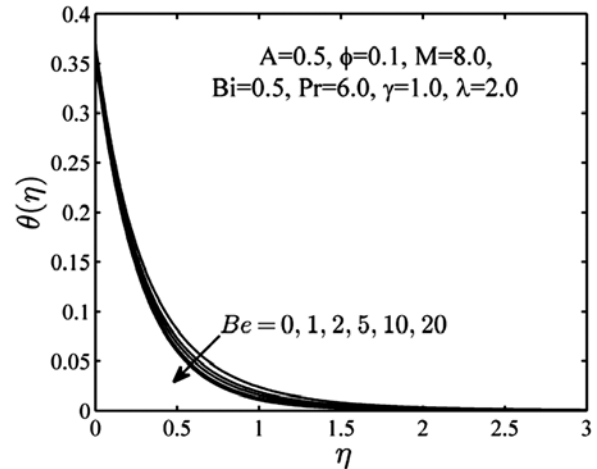

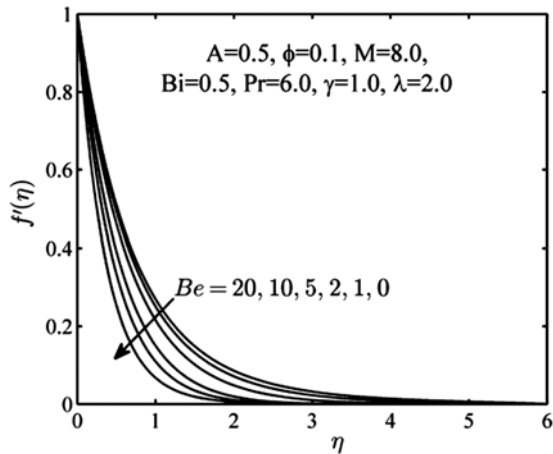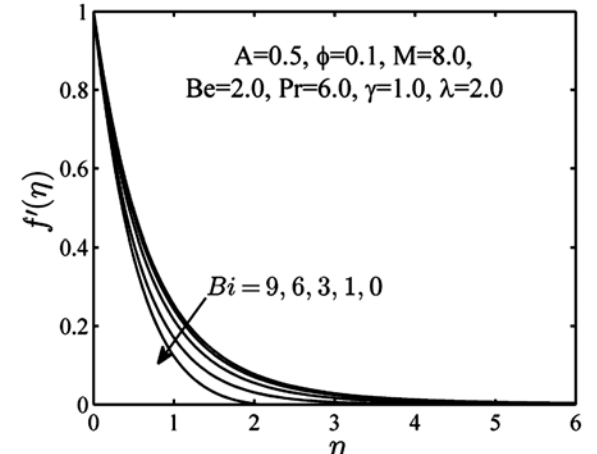Fig. 7 – Effect of ϕ on temperature profiles.

Fig. 10 – Effect of Be on temperature profiles.

Fig. 8 – Effect of Be on axial velocity profiles.

Fig. 11 – Effect of Bi on axial velocity profiles.
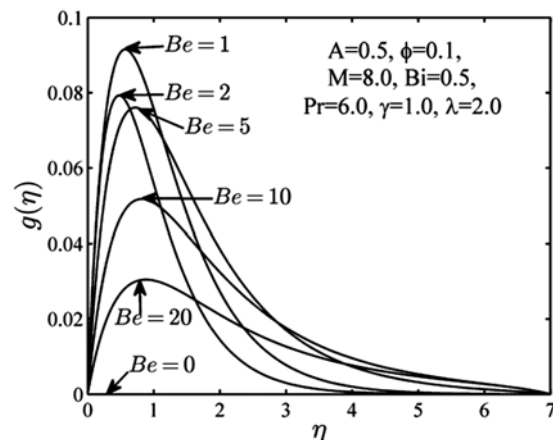
Fig. 9 – Effect of Be on transverse velocity profiles.
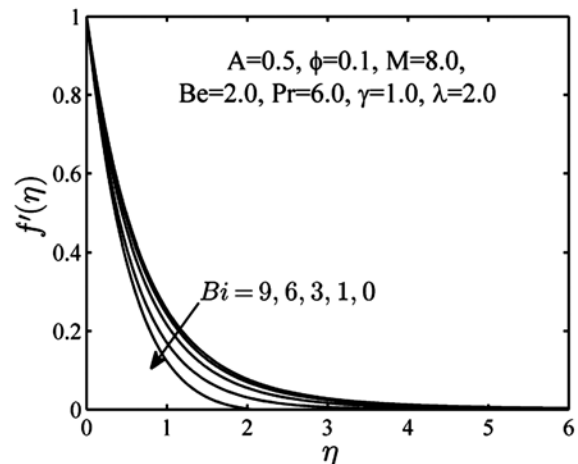
Fig. 12 – Effect of Bi on transverse velocity profiles.

increasing. This trend is contrary to the temperature distributions presented in Fig. 16. When there are no the external magnetic field in this flow, i.e., $M = 0$, the transverse velocity identically equal to zero. It

means that the cross flow in the z-direction vanishes as $M = 0$. As the external magnetic field is present, an increase in M gives rise to a greater peak value of the transverse velocity $g(\eta)$ and a thinner boundary layer of the transverse velocity.
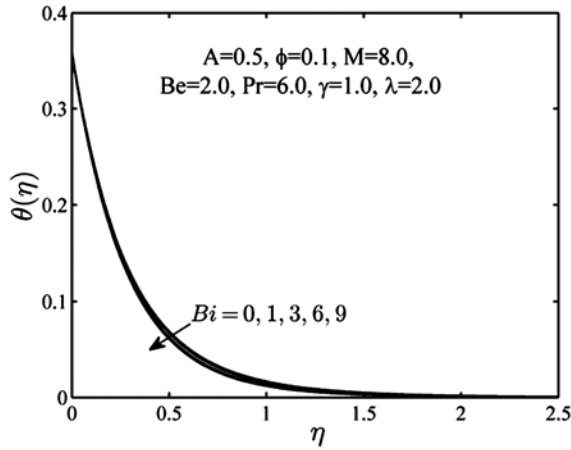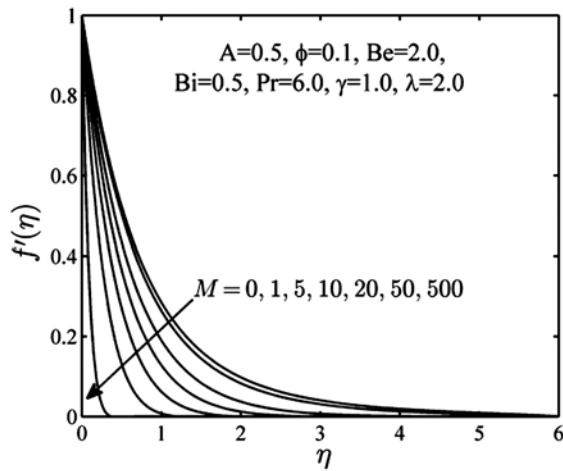
Figures 17, 18 and 19 illustrate the effects of the boundary convection parameter λ on the axial velocity $f'(\eta)$, transverse velocity $g(\eta)$ and temperature $\theta(\eta)$, respectively. From Figs 17 and 18, it is noticed that an increase in the boundary convection parameter λ will lead to a slight increase in the axial velocity $f'(\eta)$ and in the transverse velocity $g(\eta)$. However, Fig. 19 shows that the boundary convection parameter λ has significant influences on the temperature of nanofluid. The increasing value of the boundary convection parameter λ obviously increases the temperature and thickens the temperature boundary layer.

Fig. 13 – Effect of Bi on temperature profiles.
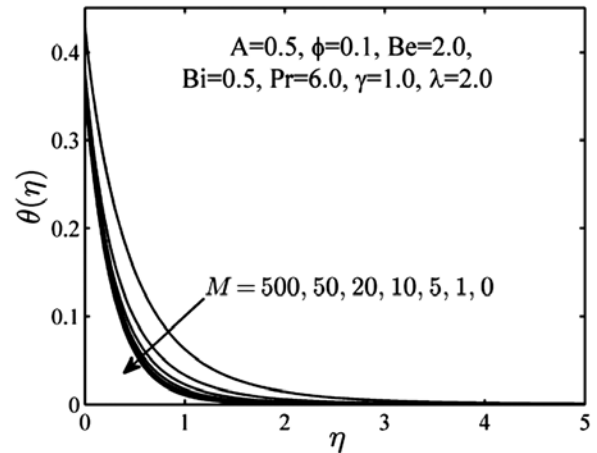

Fig. 14 – Effect of M on axial velocity profiles.
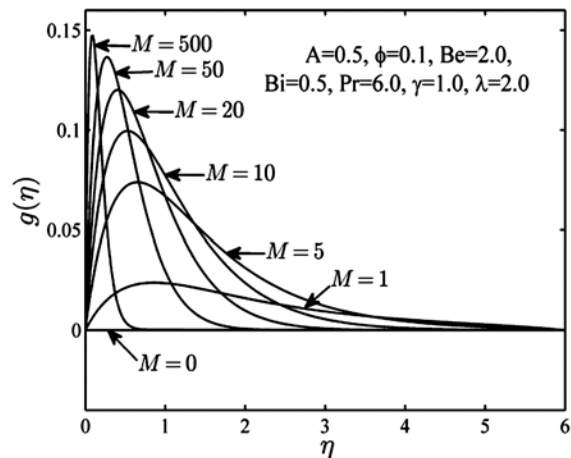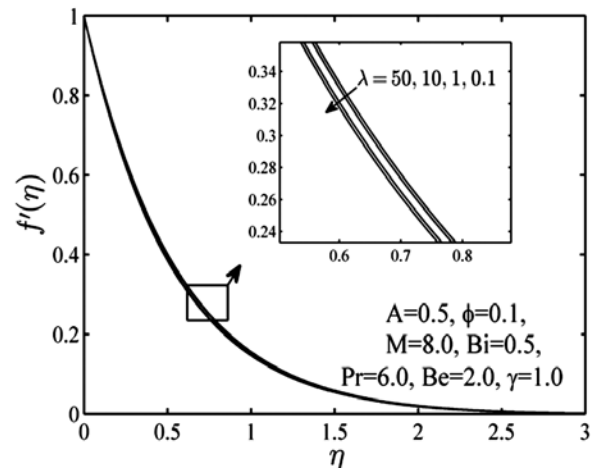

Fig. 15 – Effect of M on transverse velocity profiles.
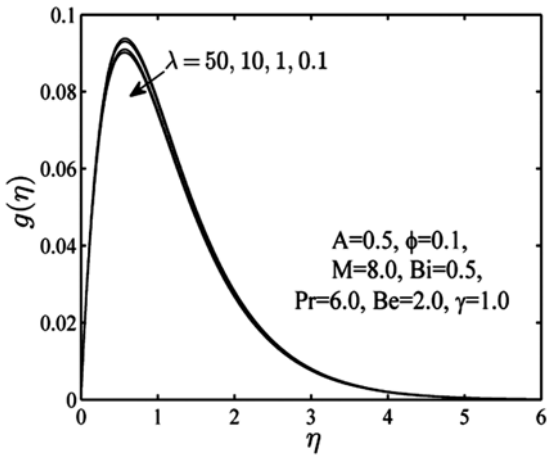

Fig. 16 – Effect of M on temperature profiles.

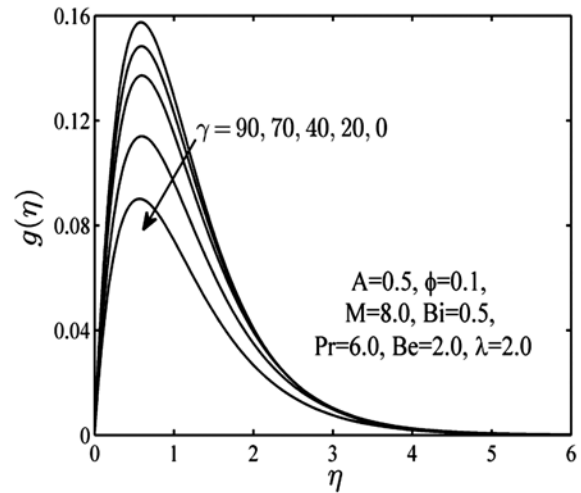Fig. 17 – Effect of λ on axial velocity profiles.

Fig. 18 – Effect of λ on transverse velocity profiles.

Fig. 19 – Effect of λ on temperature profiles.

Fig. 20 – Effect of γ on axial velocity profiles.

Fig. 21 – Effect of γ on transverse velocity profiles.

Fig. 22 – Effect of γ on temperature profiles.

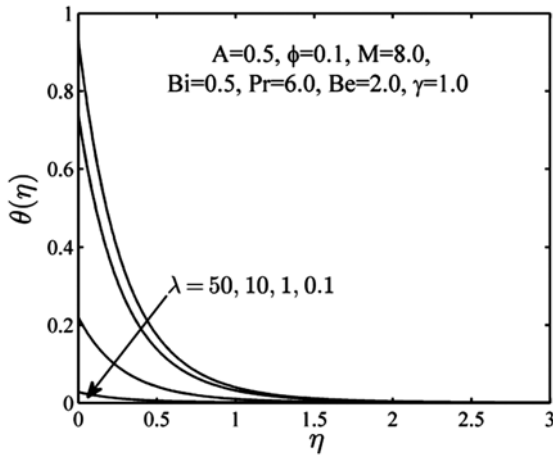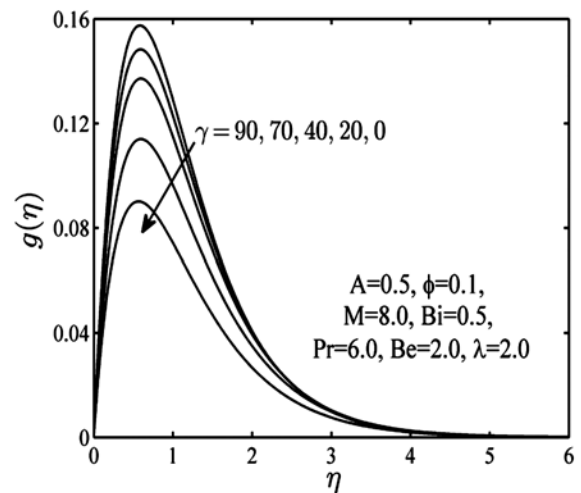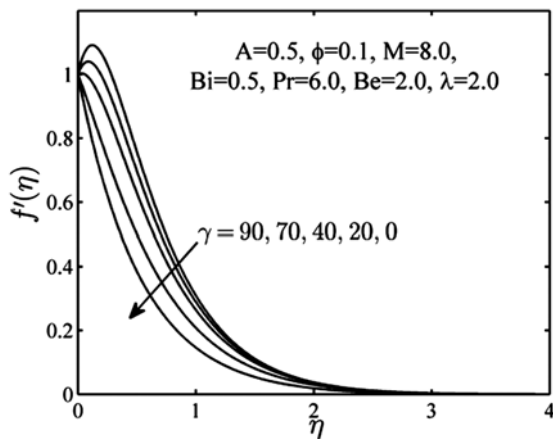Figures 20, 21 and 22 depict the profiles of the axial velocity $f'(\eta)$, the transverse velocity $g(\eta)$ and temperature $\theta(\eta)$ for different values of the mixed convection parameter γ. Figure 20 reveals that the axial velocity $f'(\eta)$ increases and gradually produces a peak value and then decays to the free stream velocity with the increase of γ. From Fig. 21, we observe that a greater value of γ brings out a higher velocity of the transverse velocity $g(\eta)$ of Cu-water nanofluid in the boundary layer. Figure 22 shows that an increase in the mixed convection parameter γ leads to the reduction of the temperature of Cu-water nanofluid.

5 Conclusions

This study has analyzed the effects of the Hall and ion-slip currents on MHD mixed convective flow and heat transfer of Cu-water nanofluid over a vertical plate. The plate surface stretches with an unsteady velocity. Numerical solutions have been obtained by using the fourth order Runge-Kutta scheme with shooting method. The following specific conclusions can be drawn:

(i)   The additive of Cu nanoparticle has significant effects on both axial and transverse velocity components. The nanofluid with higher density Cu nanoparticle provides higher heat transfer rate.

(ii)   The axial velocity of the nanofluid increases with the increasing values of the nanoparticle volume fraction, Hall parameter, ion-slip parameter, boundary convection parameter and mixed convection parameter; however, it reduces with the increasing values of unsteadiness parameter and magnetic parameter.

(iii) Temperature of nanofluid in this boundary layer is a decreasing function of unsteadiness parameter, Hall parameter, ion-slip parameter and mixed convection parameter, and it is an increasing function of the nanoparticle volume fraction, boundary convection parameter and magnetic parameter.

(iv) The transverse velocity profiles for various values of all the parameters have a common feature that they monotonically reach to a peak value and then monotonically decrease to zero.

(v)   The peak value of the transverse velocity decreases as ion-slip parameter increases, and increases with the increasing values of unsteadiness parameter, the nanoparticle volume fraction, mixed convection parameter, boundary convection parameter. It first increases and then decreases when Hall parameter increases.

(vi)   An increase in magnetic parameter makes the transverse velocity produce a greater peak value of the transverse velocity and a thinner boundary layer.

Acknowledgement

References

1   Tzou D Y, *Int J Heat Mass Trans*, 51 (2008) 2967.
2   Tzou D Y, *J Heat Trans-T ASME*, 130 (2008) 072401.
3   Alloui Z, Guiet J, Vasseur P & Reggio M, *Can J Chem Eng*, 90 (2012) 69.
4   Freidoonimehr N, Rashidi M M & Mahmud Shohel M, *Int J Therm Sci*, 87 (2015) 136.
5   Kuznetsov A V & Nield D A, *Int J Therm Sci*, 49 (2010) 243.
6   Aziz A, *Commun Nonlinear Sci Numer Simulat*, 14 (2009) 1064.
7   Aziz A & Khan W A, *Int J Therm Sci*, 52 (2012) 83.
8   Yacob N A, Ishak A, Pop I & Vajravelu K, *Nanoscale Res Lett*, 6 (2011) 1.
9   Makinde O D & Aziz A, *Int J Therm Sci*, 50 (2011) 1326.
10   Su X H, Zheng L C, Zhang X X & Zhang J H, *Chem Eng Sci*, 78 (2012) 1.
11   Subhashini S V, Sumathi R & Momoniat E, *Meccanica*, 49 (2014) 2467.
12   Yacob N A, Ishak A, Roslinda N & Pop I, *J Appl Math*, 2013 (2013) 696191.
13   Sheikholeslami M, Hatami M & Ganji D D, *Powder Technology* 246 (2013) 327.
14   Hatami M, Nouri R & Ganji D D, *J Mol Liq*, 187 (2013) 294.
15   Yazdi M E, Moradi A & Dinarvand S, *Arab J Sci Eng*, 39 (2014) 2251.
16   Sutton G W & Sherman A, *Engineering magnetohydrodynamics*, (McGraw-Hill: New York), 1965.
17   Megahed A A, Soliman R K & Ahmed A A, *Int J Nonlin Mech*, 38 (2003) 513.
18   Srnivasacharya D & Shiferaw M, *J Braz Soc Mech Sci Eng*, 30 (2008) 313.
19   Srnivasacharya D & Kaladhar K, *Commun Nonlinear Sci Numer Simulat*, 17 (2012) 2447.
20   Asghar S, Hussain Q, Hayat T & Alsaadi F, *Appl Math Mech*, 35 (2014) 1509.
21   Su X H & Zheng L C, *Cent Eur J Phys*, 11 (2013) 1694.
22   Makinde O D, Iskander T, Maboodc F, Khan W A & Tshehla M S, *J Mol Liq*, 221 (2016) 778.
23   Hayat T, Zahir H, Tanveer A & Alsaedi A, *J Magn Magn Mater*, 407 (2016) 321.
24   Hayat T, Shafique M, Tanveer A & Alsaedi A, *J Magn Magn Mater*, 407 (2016) 51.
25   Vajravelu K, Prasad K V, Lee J H, Lee C H, Pop I & Van Gorder R A, *Int J Therm Sci*, 50 (2011) 843.
26   Su X H, *Indian J Pure Appl Phy*, 53 (2015) 643.
27   Rana P & Bhargava R, *Commun Nonlinear Sci Numer Simul*, 16 (2011) 4318.